JGR Space Physics

RESEARCH ARTICLE
10.1029/2025JA034078

Diffusive and Nonlinear Scattering of Ring Current Protons by Electromagnetic Ion Cyclotron Waves in the Earth's Inner Magnetosphere

Q. Ma[1,2], W. Li[1], J. Bortnik[2], M. Hanzelka[3,4], L. Gan[1], A. V. Artemyev[5], and X.-C. Shen[1]

[1]Center for Space Physics, Boston University, Boston, MA, USA, [2]Department of Atmospheric and Oceanic Sciences, University of California, Los Angeles, CA, USA, [3]GFZ German Research Centre for Geosciences, Potsdam, Germany, [4]Department of Space Physics, Institute of Atmospheric Physics of the Czech Academy of Sciences, Prague, Czech Republic, [5]Department of Earth, Planetary and Space Sciences, University of California, Los Angeles, CA, USA

Key Points:

- Test particle simulations reveal diffusive and nonlinear scattering of 1 keV–1 MeV protons with 0–90° pitch angles by electromagnetic ion cyclotron (EMIC) waves
- Anomalous phase trapping and positive phase bunching rapidly transport protons from small pitch angles toward intermediate values
- Quasilinear diffusion becomes inaccurate, and advection begins to dominate for EMIC waves with amplitudes larger than 1 nT at $L = 5$

Correspondence to:
Q. Ma,
qma@bu.edu

Citation:
Ma, Q., Li, W., Bortnik, J., Hanzelka, M., Gan, L., Artemyev, A. V., & Shen, X.-C. (2025). Diffusive and nonlinear scattering of ring current protons by electromagnetic ion cyclotron waves in the earth's inner magnetosphere. *Journal of Geophysical Research: Space Physics*, *130*, e2025JA034078. https://doi.org/10.1029/2025JA034078

Received 13 APR 2025
Accepted 16 JUL 2025

Abstract We evaluate the diffusive and nonlinear scattering of ring current protons by electromagnetic ion cyclotron (EMIC) waves in the Earth's inner magnetosphere using test particle simulations. EMIC waves are commonly observed inside and outside the plasmasphere with wave amplitudes ranging from 100 pT to several nT. Field-aligned EMIC waves can scatter 1 keV–1 MeV protons counter-streaming with respect to the waves through first order cyclotron resonance. Through the analyses of the proton equatorial pitch angle variations along the field line, our simulations reveal the typical interaction features including quasilinear diffusion for small wave amplitudes, phase trapping and bunching at intermediate and large pitch angles, anomalous phase trapping and positive phase bunching at small pitch angles, and non-resonant scattering at pitch angles and energies outside the resonance regime. Using different wave amplitudes from 100 pT to 5 nT, we compared the modeling results of proton equatorial pitch angle variations between quasilinear and test particle simulations, and between diffusive scattering and advective effects. For monochromatic He-band EMIC waves at $L = 5$, the interaction between protons and EMIC waves with amplitudes below 500 pT could be described as a diffusive process and quantified by quasilinear theory; nonlinear interactions and advection effects become important for wave amplitudes larger than 1 nT. The interactions between EMIC waves and ring current protons are analogous to the interactions between whistler-mode chorus waves and radiation belt electrons described in previous studies, despite the quantitative differences in the wave amplitude threshold of quasilinear diffusion applicability.

1. Introduction

Satellite missions in the Earth's magnetosphere commonly observe large amplitude electromagnetic ion cyclotron (EMIC) waves during geomagnetic storms (e.g., Meredith et al., 2014; Remya et al., 2023). Hot ions in the ring current undergo energy-dependent drifts around the Earth due to the electric and magnetic fields, and a temperature anisotropy gradually develops over the dusk to the dayside sectors (Daglis et al., 1999; Jordanova et al., 1997). The velocity distribution of hot ions is unstable, leading to the generation of the left-hand polarized EMIC waves in the frequency bands between the ion gyrofrequencies of different species (Chen et al., 2009; Gary et al., 1995; Jordanova et al., 2001; Min et al., 2015). Wave generation is most efficient along or anti-parallel to the magnetic field direction near the magnetic equator. As the waves propagate from the equator to higher latitudes, the left-hand polarized waves could travel through the latitude of wave crossover frequency and become right-hand polarized (Allen et al., 2015; Hanzelka, Li, Ma, et al., 2023), and subsequently, some EMIC waves could be detected on the Earth's surface by ground-based magnetometers (Engebretson et al., 2018; Fraser, 1985; Jacobs, 1970; Usanova et al., 2014).

EMIC waves play a significant role in the rapid dropout and gradual decay of radiation belt electrons (Drozdov et al., 2020; Lyu et al., 2024). The electron resonant energy can be reduced to below 1 MeV due to EMIC waves observed in the high-density region of the outer plasmasphere or the plasmaspheric plumes (Capannolo et al., 2018, 2019; Qin et al., 2025; Zhang et al., 2014, 2016). As these regions overlap with the region of high fluxes of relativistic electrons in the outer radiation belt, EMIC waves can cause efficient pitch angle scattering and loss of MeV electrons during the recovery phase of geomagnetic storms (e.g., Ma et al., 2016). EMIC wave

scattering has been demonstrated to be a dominant MeV electron loss mechanism in addition to magnetopause shadowing, which requires high solar wind pressure (Staples et al., 2023).

Quasilinear theory has been traditionally used to model the electron scattering by EMIC waves in the radiation belts (Ni et al., 2015). The quantification of electron loss as a diffusive scattering process has been validated by comparing with satellite observations of electron flux variations (Drozdov et al., 2017; Ma et al., 2015; Shprits et al., 2016). However, because the EMIC wave amplitude could reach several nT, corresponding to a few percent of the background magnetic field at the equator, the applicability of the quasilinear theory remains controversial. Test particle simulations (Bortnik et al., 2022; Hanzelka, Li, & Ma et al., 2023, Hanzelka, Li, & Ma, 2023) revealed nonlinear interaction features of relativistic electrons due to EMIC waves, including non-resonant scattering, positive advection due to force bunching, and negative advection due to phase trapping, in addition to the quasilinear diffusion effects. The importance and incorporation of nonlinear effects in global radiation belt modeling is thus an area that remains under active research.

Recent satellite observations and modeling demonstrated the importance of EMIC waves in ion dynamics in the ring current system, including the ion flux dropout and decay at tens of keV to several hundred keV energies (e.g., Lyu et al., 2022), ion precipitation to the upper atmosphere (e.g., Miyoshi et al., 2008; Ni et al., 2023), and heating of thermal and suprathermal ion populations (Anderson & Fuselier, 1994; Horne & Thorne, 1990; Keika et al., 2013; Mouikis et al., 2002). In addition, EMIC-induced precipitation of hot protons from the magnetosphere to the atmosphere could cause isolated subauroral proton arcs that appear equatorward of the main auroral oval (Frey et al., 2004; Immel et al., 2002; Jordanova et al., 2007; Sakaguchi et al., 2012; Spasojevic et al., 2004; Zhang, Y. et al., 2005). Through resonant interactions with ions of different energies, EMIC waves thus mediate the energy transfer from ring current ions to lower energy ions or other species (Liu et al., 2022; Ma et al., 2019; Thorne & Horne, 1994).

Global modeling of ring current proton scattering by EMIC waves usually adopts quasilinear theory (e.g., Cao et al., 2016, 2019), which assumes that the waves are broadband, incoherent, and much weaker than the background magnetic field, such that each individual interaction with a charged particle is linear. However, it is known that occasionally EMIC waves are not incoherent and in fact coherent rising tone structures of EMIC waves have been observed by satellites in the Earth's magnetosphere (Blum et al., 2021; Clilverd et al., 2015; Nakamura et al., 2019; Shoji et al., 2018; Sigsbee et al., 2023). Previous studies (Bortnik et al., 2010; Shoji et al., 2021; Wang et al., 2017; Zhu et al., 2012) reported the phase trapping and phase bunching of protons at intermediate to large pitch angles by coherent EMIC waves, inducing significant advection effects in addition to diffusive scattering. The phase trapped protons remain in resonance with the EMIC waves for an extended period, so that their equatorial pitch angles increase significantly when they stream through the wave fields. The phase bunched protons are clustered near the resonance location, experience one resonance with the waves, and have similar trajectories with some scattering in the equatorial pitch angles. Multiple parameters determine the nonlinear effects of EMIC waves, including the proton initial energy, pitch angle, and resonant latitude (Su et al., 2014; Zhou & Cai, 2024).

In this study, we evaluate the diffusive and nonlinear scattering of protons induced by EMIC waves in the full pitch angle range of 0°–90° and the energy range of 1 keV–1 MeV using test particle simulations. Our methodology and assumptions are described in Section 2. The monochromatic He-band EMIC waves are launched from the equator to higher latitudes, scattering the protons which travel toward the magnetic equator. The results of our test particle simulations are presented in Section 3. The typical features of proton scattering are revealed, and the wave amplitude dependence of nonlinear effects is evaluated. Section 4 evaluates proton probability density functions due to interactions with EMIC waves. In Section 5, the major results of our paper are summarized and discussed.

2. Analysis Method of Proton Scattering by EMIC Waves

The motion of protons interacting with EMIC waves can be described by the momentum equation (Bell, 1984; Bortnik et al., 2008; Inan et al., 1978):

$$\frac{d\mathbf{p}}{dt} = q\left(\mathbf{E}_w + \frac{\mathbf{p}}{\gamma m} \times (\mathbf{B}_w + \mathbf{B}_0)\right), \quad (1)$$

where t is the time, $\mathbf{p}$, q, and m are the proton momentum, charge, and mass respectively, γ is the Lorentz factor, $\mathbf{E}_w$ and $\mathbf{B}_w$ are the wave electric and magnetic fields respectively, and $\mathbf{B}_0$ is the Earth's magnetic field. We use the gyro-averaged equations of motions from Li et al. (2015) and Fu et al. (2016) to numerically solve Equation 1 following the proton trajectory along the field line. Although relativistic effects are considered in our simulations, the ring current protons at 1 keV–1 MeV energies are not relativistic ($\gamma \approx 1$).

The resonance condition is satisfied when the harmonics of the proton gyrophase change at the same rate as the doppler-shifted wave phase:

$$\omega - k_{\parallel} v_{\parallel} - N\frac{\omega_{cp}}{\gamma} - N\frac{\frac{dP_{\theta,w}}{dt}}{P_{\perp}} = 0, \tag{2}$$

where ω is the wave angular velocity, $k_{\parallel}$ is the wave vector parallel to $\mathbf{B}_0$, $v_{\parallel}$ is the proton velocity parallel to $\mathbf{B}_0$, $P_{\perp}$ is the proton momentum perpendicular to $\mathbf{B}_0$, N is the resonance harmonic number, $\omega_{cp} = \frac{qB_0}{m}$ is the proton cyclotron frequency due to $\mathbf{B}_0$, and $dP_{\theta,w}/dt$ is the rate of proton momentum change in the direction of proton gyrophase due to the waves. Assuming that the $\frac{dP_{\theta,w}/dt}{P_{\perp}}$ term is small, the resonance condition is simplified to the form $\omega - k_{\parallel} v_{\parallel} = N\frac{\omega_{cp}}{\gamma}$, which is same as the resonance condition in quasilinear modeling. The protons counter-streaming with EMIC waves satisfy the cyclotron resonance ($N = 1$) condition.

The EMIC waves are launched from the magnetic equator and propagate to the northern hemisphere at $L = 5$. The EMIC wave frequency is $\omega = 0.8\omega_{cHe,eq}$, where $\omega_{cHe,eq}$ is the Helium gyrofrequency at the equator. This frequency is close to the frequency of peak wave intensity of He-band EMIC waves (Zhang et al., 2016), which are commonly observed in the high-density regions. The total electron density at the equator ($N_{e,eq}$) is taken to be 118 cm^{-3} based on the plasmaspheric density model by Sheeley et al. (2001). The density changes as a function of latitude (λ) as $N_e = N_{e,eq}\cos^2\lambda$, simplified from the model by Denton et al. (2002). The wave normal angle was 0°. The ion plasma is assumed to be composed of 90% H^+, 5% He^+, and 5% O^+. The latitude of the local crossover wave frequency is thus located at ~12.7°. The wave amplitude is assumed to decrease before reaching the latitude of crossover wave frequency as $B_w = B_{w,eq}(\tanh(10 - \mathrm{Lat}) + 1)/2$, where Lat is the latitude in degree. The protons are launched from their mirror points to the magnetic equator. We set 89 equatorial pitch angle grids evenly spaced from 1° to 89° and an additional pitch angle at 89.5°, 37 energy grids evenly spaced in the logarithmic space from 1 keV to 1 MeV, and 72 gyrophase grids evenly spaced from 0° to 354°. In total, 239,760 protons were traced until they reached the magnetic equator.

An example of protons interacting with EMIC waves is shown in Figure 1a for the protons with an initial equatorial pitch angle (α_{eq}) of 10° and energy (E) of 14.68 keV. The EMIC wave amplitude profile is overplotted as the blue dashed curve ($B_{w,eq} = 2$ nT). The wave amplitude is close to 2 nT from the equator to 8° latitude and gradually decreases to ~0 nT as the latitude increases to 12°. This wave amplitude profile reduces non-resonant scattering of protons entering the wave fields from >12° latitudes, which is caused by the gradient of EMIC wave fields (An et al., 2024), following the approach used by Bortnik et al. (2022). The protons experience positive phase bunching by EMIC waves, resulting in a systematic increase of equatorial pitch angles with a spreading between 17° and 37°. Figure 1b shows the proton pitch angle distribution as a function of the gyro interaction phase when the protons travel to the equator. The protons are clustered into the phase range of 37°–160° with the average of the scattered pitch angles higher than the initial pitch angle, suggesting an advection effect.

Using the resultant proton pitch angle distributions at the magnetic equator, we evaluate the scattering effect as the diffusion coefficient $\langle D_{\alpha\alpha}\rangle = \left\langle\frac{(\Delta\alpha - <\Delta\alpha>)^2}{2\Delta t}\right\rangle$ and the average drift effect as the drift coefficient $A_{\alpha} = \left\langle\frac{\Delta\alpha}{\Delta t}\right\rangle$, where $\Delta\alpha$ is the equatorial pitch angle change from the mirror point to the equator, Δt is half of the proton bounce period, and $\langle\ldots\rangle$ represents the average over different initial wave-particle phases. The drift term is contributed by the proton advection and the pitch angle gradient of $\langle D_{\alpha\alpha}\rangle$ (Allanson et al., 2022). The diffusion and drift coefficients from test particle simulations are shown in Figures 1d and 1e. As a comparison, we also calculate the quasilinear diffusion coefficients using the Full Diffusion Code for EMIC waves (Ma et al., 2019) in Figure 1c. The wave and background parameters in the quasilinear calculation are the same as those in the test particle simulations. The

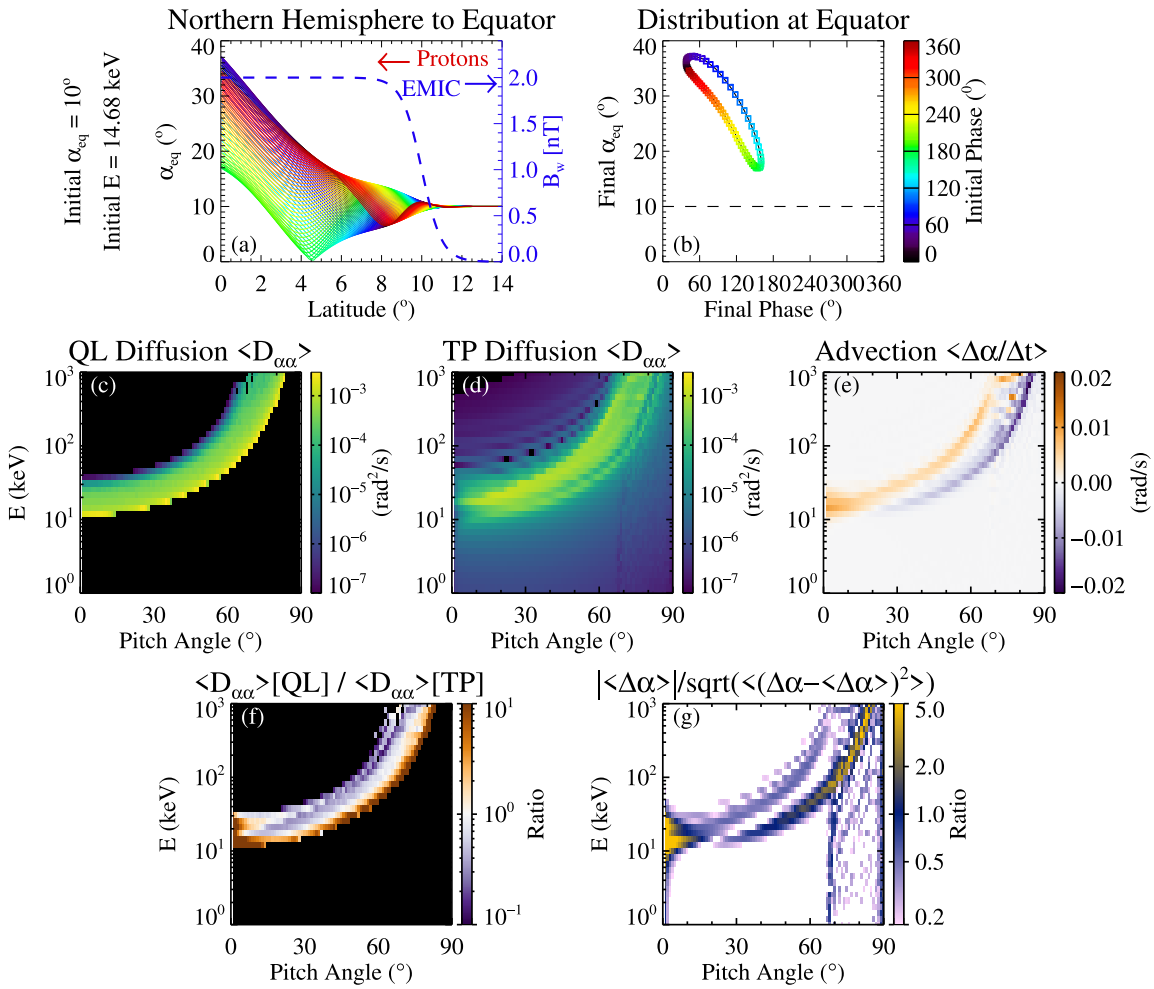

Figure 1. Test particle simulations of proton scattering by He-band EMIC waves at $L = 5$. (a) Variations of proton equatorial pitch angle as the protons travel from high latitude to the equator and resonate with EMIC waves propagating from equator to high latitudes. The initial equatorial pitch angle is 10° and initial energy is 14.68 keV. The solid lines with different colors represent protons with different initial phases. The blue dashed line is the EMIC wave amplitude distribution. (b) Proton pitch angle as a function of their gyro interaction phase at the magnetic equator. The initial equatorial pitch angle is marked as a dashed horizontal line. (c) Bounce-averaged pitch angle diffusion coefficients as a function of proton energy and equatorial pitch angle calculated using quasilinear (QL) theory. (d) Proton pitch angle diffusion coefficients calculated from test particle (TP) simulation results. (e) Proton drift coefficients calculated from test particle simulation results. (f) Ratio between the diffusion coefficients from quasilinear theory and test particle simulations. (g) Ratio between the drift and diffusion effects, evaluated as the mean changes in proton equatorial pitch angle and the standard deviation of the pitch angle changes.

black area in Figure 1c indicates the pitch angles and energies where the resonance condition cannot be satisfied. The majority of the scattering and advection effects are found within the resonance regime.

The ratio between the quasilinear diffusion coefficients and test particle diffusion coefficients is calculated in Figure 1f to evaluate the applicability of quasilinear theory in describing the proton interaction with EMIC waves. The brown and purple colors suggest that the quasilinear theory over- and under-estimate the scattering effects, respectively, while the white color indicates agreement between the two methods. The importance of drift is evaluated as the ratio between the average pitch angle changes and the standard deviation of pitch angle changes ($\frac{|<\Delta\alpha>|}{\sqrt{<(\Delta\alpha-<\Delta\alpha>)^2>}}$). As shown in Figure 1g, a low ratio (e.g., below 0.5) indicates that the interactions could be described as scattering around the initial equatorial pitch angle, and the ratio above one indicates a significant drift in the average pitch angle distribution. We will discuss the different regimes of typical proton scattering features in Section 3.

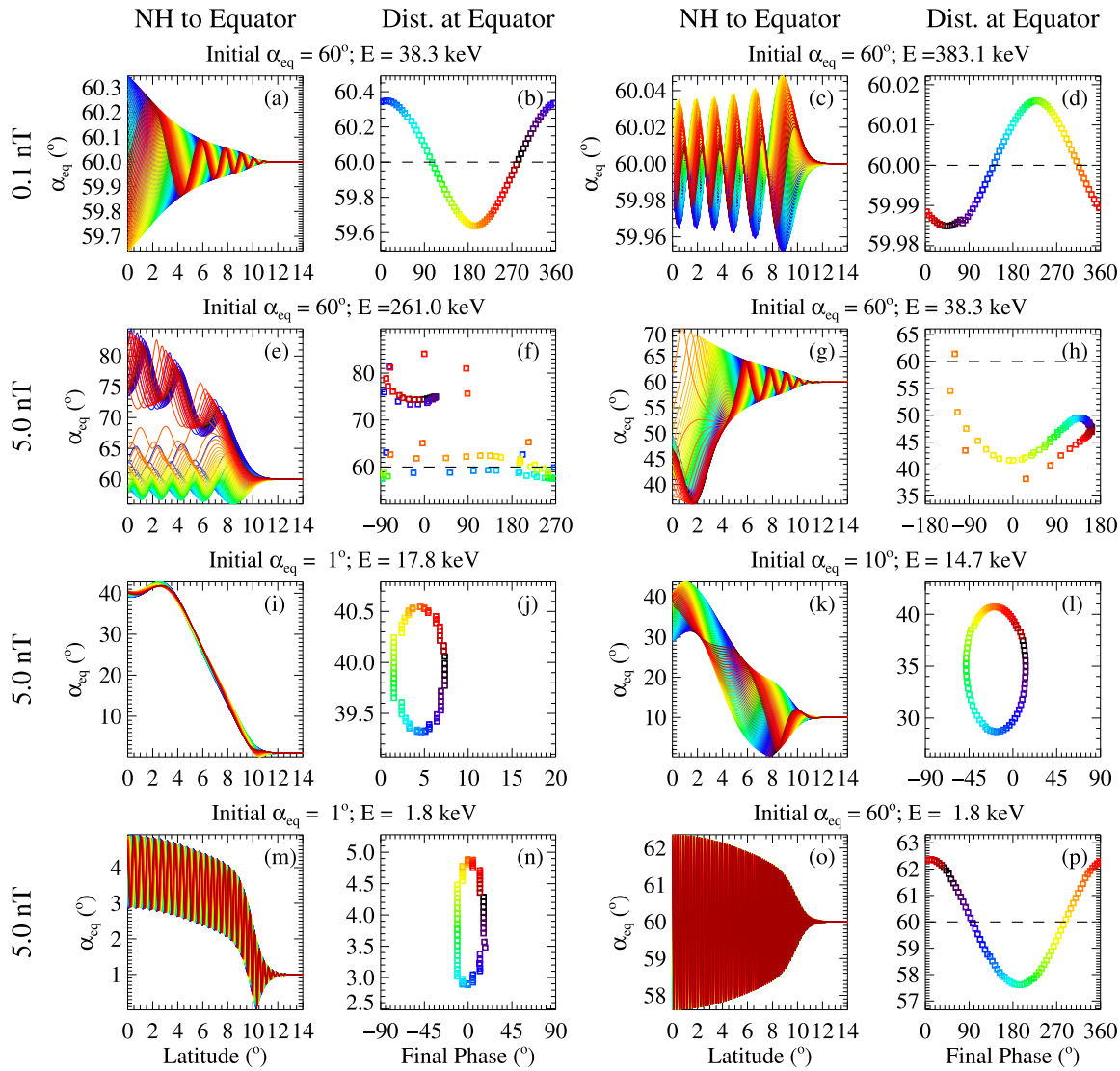

Figure 2. Typical proton equatorial pitch angle variations during the interaction with EMIC waves. The figure format is the same as Figures 1a and 1b for each case. (a–b) Quasilinear diffusion and (c–d) non-resonant scattering of protons due to weak EMIC waves with 0.1 nT amplitude. (e–f) Phase trapping, (g–h) phase bunching, (i–j) anomalous phase trapping, and (k–l) positive phase bunching of protons due to resonant interaction with 5 nT EMIC waves. (m–n) Positive phase bunching and (o–p) scattering of protons at energies below the minimum resonance energy due to 5 nT EMIC waves. The initial proton equatorial pitch angle and energy are labeled for each case.

3. Proton Scattering Features and Wave Amplitude Dependence

We examined the proton pitch angle variations that occur during their interactions with EMIC waves of different wave amplitudes ranging from 0.1 to 5 nT. Figure 2 summarizes the typical proton scattering features resulting from small wave amplitudes of 0.1 nT (row 1) and large wave amplitudes of 5 nT (rows 2–4). For small wave amplitude, and interactions taking place inside the resonance regime, the protons are scattered approximately symmetrically around the initial pitch angle (Figures 2a and 2b). Weak scattering is also found for the pitch angles and energies outside the resonance regime as the protons enter the wave fields (Figures 2c and 2d).

Nonlinear effects become significant for an EMIC wave amplitude of 5 nT. In Figures 2e and 2f, some protons are phase trapped by EMIC waves and experience an extended resonant interaction path, resulting in a significant increase in their equatorial pitch angles. For the case of lower proton energy and moderate pitch angles in Figures 2g and 2h, the protons are phase bunched and drift toward lower equatorial pitch angles. Similar phase trapping and bunching cases have been analyzed in previous studies (e.g., Zhu et al., 2012). At very low equatorial

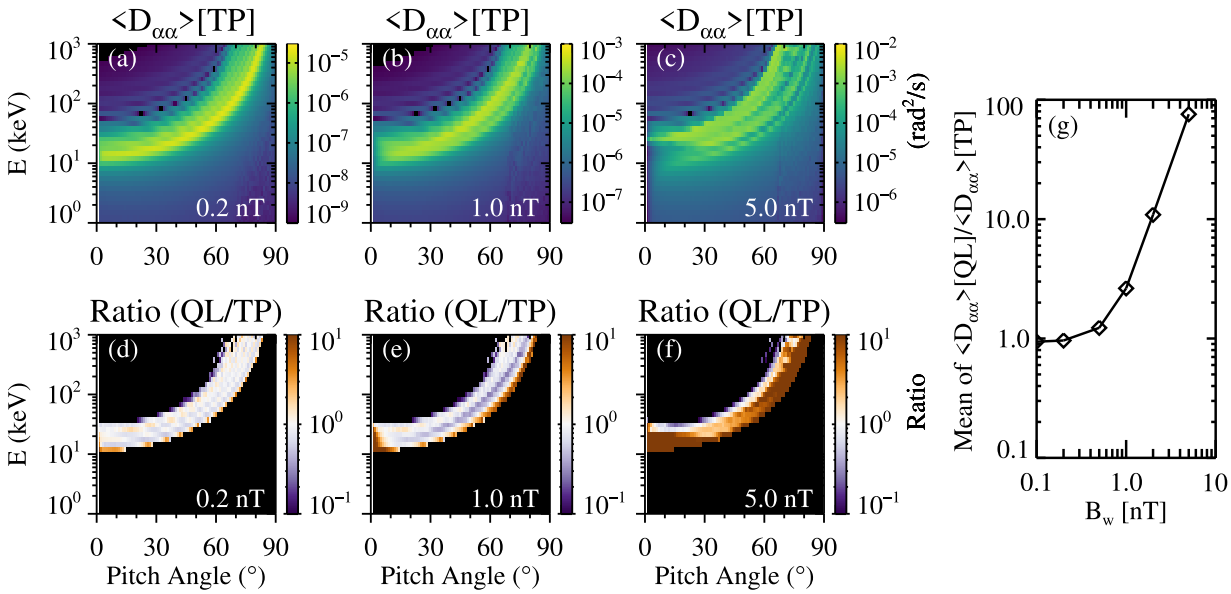

Figure 3. Diffusion coefficients from test particle (TP) simulations and the comparison with quasilinear (QL) modeling at $L = 5$. (a–c) Diffusion coefficients as a function of proton pitch angle and energy calculated using test particle simulations with different wave amplitudes. (d–f) Ratio of diffusion coefficients between quasilinear modeling and test particle simulation results. (g) Mean value of the diffusion coefficient ratios as a function of wave amplitude within the resonance regime.

pitch angles (i.e., 1°, Figures 2i and 2j), protons experience anomalous phase trapping, during which the equatorial pitch angles jump to above 39°. The protons that were initially inside the loss cone became stably trapped in the magnetosphere after such interactions, preventing them from precipitating into the atmosphere. At 10° equatorial pitch angle (Figures 2k and 2l), protons experience positive phase bunching with pitch angles drifting to above 28°. The positive phase bunching transports protons from small pitch angles to intermediate pitch angles, potentially reducing the proton precipitation compared to the results expected from quasilinear modeling. The nonlinear proton scattering at small pitch angles due to EMIC waves is analogous to the electron scattering at small pitch angles due to chorus (Albert et al., 2021; Artemyev et al., 2021; Gan et al., 2023, 2025; Kitahara & Katoh, 2019); therefore, the same terminology is used in the above descriptions. However, the proton phases due to anomalous phase trapping are clustered into a small phase range of 1.5°–7.4° (Figure 2j), showing a similar trend to that of positive phase bunching (Figure 2l).

Figures 2m–2p show the proton scattering at an energy (1.8 keV) that is below the minimum resonance energy (~10 keV). The protons could be scattered through non-resonant scattering, as shown in Figures 2o and 2p. In addition, protons at 1° pitch angle experience positive phase bunching effects outside the resonance regime (Figures 2m and 2n). However, the magnitudes of scattering and advection are small compared to the variations inside the resonance regime. Non-resonant scattering is induced when particles enter the wave fields or when particles are launched within the wave fields. As a result, the scattering and advection magnitudes depend on the setup of the wave fields and the gradients.

We calculated the diffusion coefficients and drift coefficients for the EMIC wave amplitudes of 0.1–5 nT. Figure 3 shows the diffusion coefficient comparison between test particle simulations and quasilinear theory. For 0.2 nT wave amplitude (Figures 3a and 3d), the diffusion coefficient ratios are close to one inside the resonance regime, suggesting that the proton scattering could be well quantified by quasilinear diffusion. Although the scattering from test particle simulations extends to broader pitch angles and energy ranges, the diffusion coefficients are small outside the resonance regime. At 1 nT wave amplitude (Figures 3b and 3e), the diffusion coefficients from test particle simulations are much smaller than the quasilinear modeling at small pitch angles close to 0° due to anomalous phase trapping. Near the minimum resonance energies for different pitch angles, the quasilinear modeling also overestimates the diffusion effects. At 20–80° pitch angles and energies well above the minimum resonance energy (e.g., 60° pitch angle and ~60 keV energy), the quasilinear modeling slightly underestimates the proton scattering due to the moderate phase bunching effects. At 5 nT wave amplitude, the diffusion coefficient distribution (Figure 3c) significantly deviates from the quasilinear modeling results

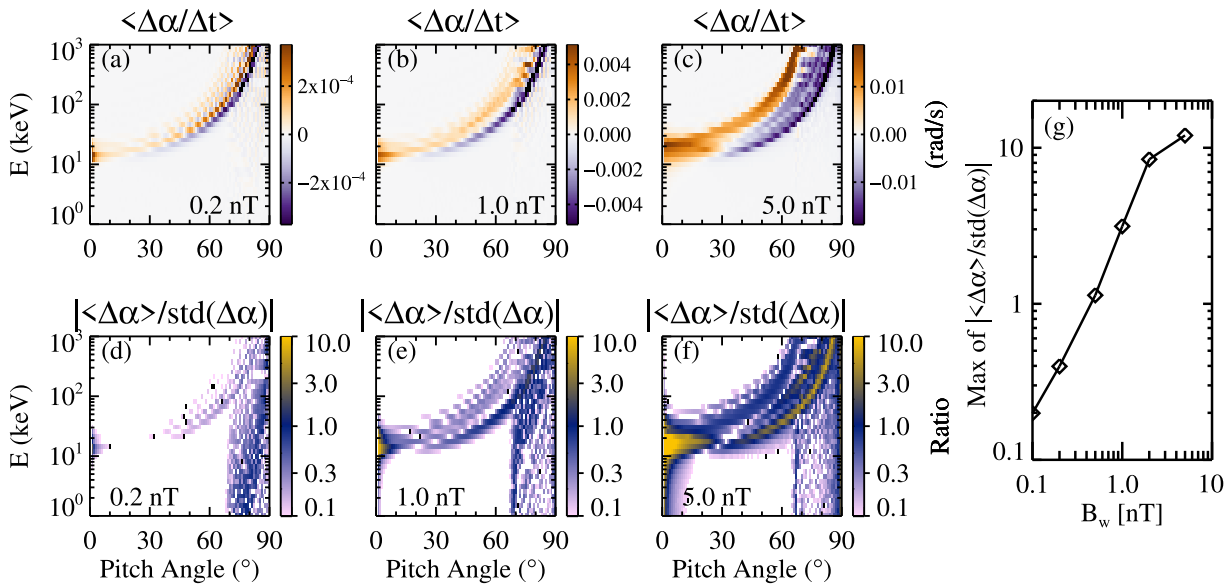

Figure 4. Drift coefficients and the comparison between drift and diffusion effects from test particle simulations at $L = 5$. (a–c) Drift coefficients as a function of proton pitch angle and energy for different EMIC wave amplitudes. (d–f) Ratio between the average and the standard deviation of equatorial pitch angle changes, to evaluate the importance of drift and diffusion effects. (g) Maximum of the drift to diffusion ratios outside the bounce loss cone within the resonance regime as a function of wave amplitude.

(Figure 1c, scaled by B_w^2). The diffusion coefficient ratio (Figure 3f) suggests that the quasilinear theory significantly overestimates the scattering effects by more than a factor of 10 inside the resonance regime. The mean value of the diffusion coefficient ratio for the pitch angles and energies in the resonance regime is plotted as a function of B_w in Figure 3g. The ratio overall increases with increasing wave amplitude. Our simulations indicate that quasilinear modeling is applicable to wave amplitudes below 0.5 nT but overestimates proton scattering for wave amplitudes above 1 nT.

Figure 4 presents the drift coefficients and the ratio between the drift and diffusion effects, quantified using the ratio between the average and standard deviation values of pitch angle changes. The drift coefficients in Figures 4a–4c present positive drift effects close to 0° pitch angles due to anomalous phase trapping, at small pitch angles (below 20°–25°) due to positive phase bunching, and at intermediate to large pitch angles (25°–80°) due to phase trapping, as well as negative drift effects at higher pitch angles (30°–90°) or lower energies (below the phase trapping energy) due to phase bunching.

The ratio between drift and diffusion is small for 0.2 nT wave amplitude (Figure 4d), suggesting that the proton variation could be well described as a diffusive process. The moderate ratios at >70° pitch angle below the minimum resonance energy (e.g., 80° pitch angle and 1 keV energy) are induced by the fact that these protons are launched within the EMIC wave fields. However, their drift coefficients are small.

At 1 nT wave amplitude (Figure 4e), the drift becomes most significant at pitch angles below 10°, induced by anomalous phase trapping and positive phase bunching. The proton variations at larger pitch angles could still be described as a diffusion process, except for the regime of phase bunching with moderate advection effects.

At 5 nT wave amplitude (Figure 4f), the ratio becomes large for most of the pitch angles and energies, suggesting that the proton pitch angle changes due to drift are much more significant than those due to diffusion. The maximum of the drift to diffusion ratios outside the bounce loss cone within the resonance regime is plotted as a function of wave amplitude in Figure 4g. The ratios are overall below 1.2 for wave amplitudes below 0.5 nT and above 3 for wave amplitudes above 1 nT, which represents a threshold for non-negligible advection effects.

4. Proton Probability Density Functions Due to EMIC Waves

We evaluated the first and second moments of the proton probability distributions of pitch angle changes as the drift and diffusion coefficients. If the distribution function of pitch-angle change has a single peak and negligible

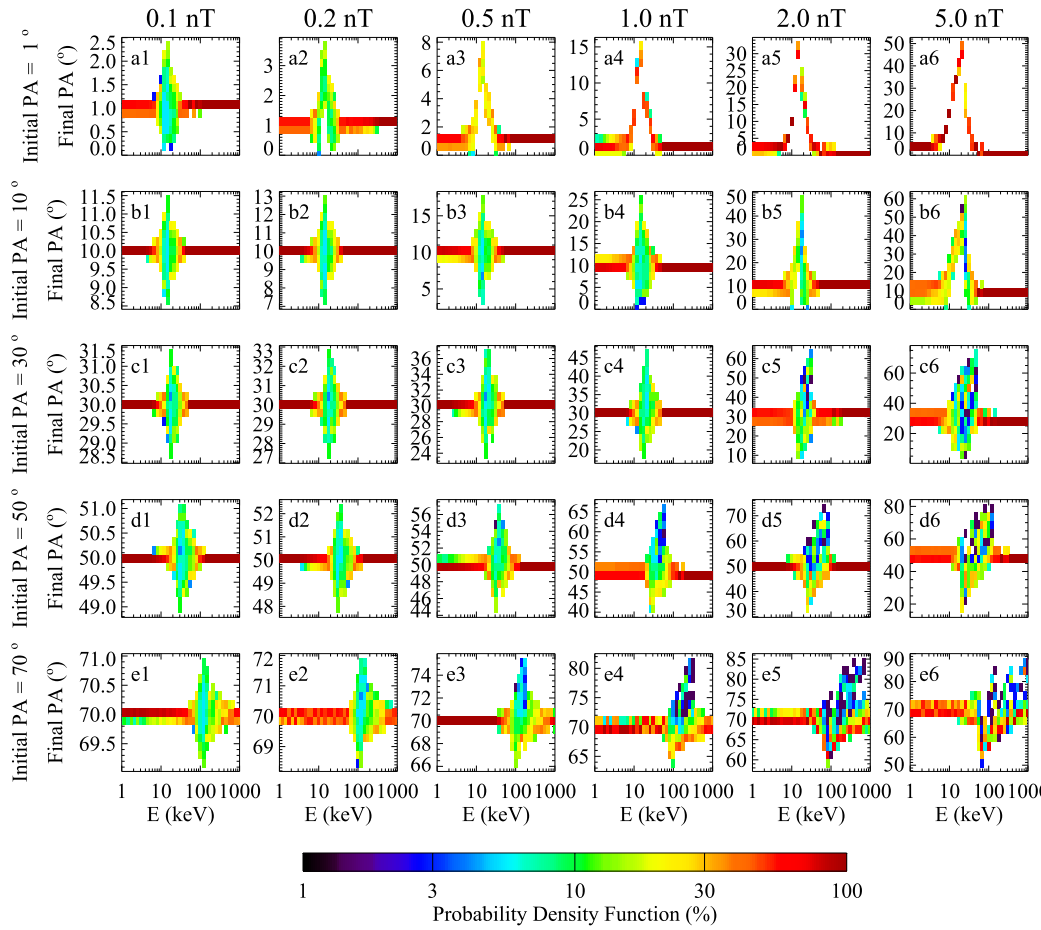

Figure 5. Probability density functions of protons with different initial energies (*x*-axis) as a function of their final pitch angle (*y*-axis) from test particle simulations. Different rows show the results for different initial pitch angles, and different columns show the results for different EMIC wave amplitudes.

probability to have change much larger than the peak value, these coefficients could approximate the average net change and spread in the proton pitch angle distributions after interacting with EMIC waves. However, the test particle trajectories in Figure 2 suggest that the proton distribution function contains a finite probability of large pitch-angle changes. The probabilistic approach should be used to accurately include such large changes caused by nonlinear resonant effects, as shown in the previous studies using the numerical Green's function approach (Omura et al., 2015), the mapping technique (Artemyev et al., 2022), or the backward Liouville mapping approach (Hanzelka et al., 2025).

Using the numerical results, we calculate the probability distribution functions of protons after their interaction with EMIC waves. This function indicates the probability of protons scattered into a final pitch angle bin for each initial proton pitch angle and energy. Figure 5 shows the probability densities as a function of proton final pitch angle for different EMIC wave amplitudes, initial pitch angles and initial energies. Consistent with the typical proton scattering features in Figure 2, the proton distribution functions are localized around the mean value of the final pitch angle in the regimes of quasilinear diffusion and non-resonant scattering. However, in the regimes of phase trapping and phase bunching, some protons are trapped to high pitch angles while a larger number of protons are phase bunched to low pitch angles (Panels c5 and c6, d3–d6 and e2–e6 in Figure 5). Large net pitch angle changes also occur at small pitch angles (Panels a2–a6 and b4–b6). Thus, the probability distribution function has a finite probability of very large pitch angle changes in these resonance regimes for sufficiently large wave amplitudes. The probability distribution functions obtained from our numerical simulations may be used to simulate the evolution of proton phase space density distribution due to nonlinear interactions with EMIC waves in the future.

5. Summary and Discussion

Large amplitude (i.e., few nT) EMIC waves are frequently observed in the Earth's magnetosphere and can potentially cause nonlinear scattering and pitch angle drift of ring current protons, resulting in pitch angle variations of protons that are different from the quasilinear modeling. We performed a series of test particle simulations at $L = 5$ to assess the proton pitch angle variations when they counter-stream with monochromatic He-band EMIC waves along the field line. The typical proton scattering features are revealed by examining the equatorial pitch angle variations over 0–90° pitch angle and 1 keV–1 MeV energy ranges. The simulation results are compared with quasilinear modeling results, and the drift effects are compared with the variation due to diffusive scattering. The main conclusions from our analyses are:

- Due to interaction with EMIC waves, the typical features of proton pitch angle variation include quasilinear diffusion for small wave amplitudes, phase trapping and bunching at intermediate and large pitch angles for large wave amplitudes, anomalous phase trapping and positive phase bunching at small pitch angles, and nonresonant scattering at pitch angles and energies outside the resonance regime.
- Anomalous phase trapping and positive phase bunching efficiently transport protons from small pitch angles to intermediate pitch angles. When the wave amplitude is sufficiently strong, these effects extend to broader pitch angle ranges from 0° to much larger than the loss cone pitch angle. Consequently, the proton precipitation may be reduced due to nonlinear interactions (Gan et al., 2023).
- Using the simulation parameters of our study, the proton scattering by EMIC waves with amplitudes below 0.5 nT at $L = 5$ could be accurately described by quasilinear diffusion. Although nonlinear scattering could occur outside the resonance regime, the effects are much weaker than the scattering due to resonant interactions, and their advection effects are not significant compared to diffusion.
- For EMIC waves with amplitudes above 1 nT at $L = 5$, the quasilinear theory generally overestimates the diffusion coefficients, and advection effects are more significant than diffusion. As wave amplitude increases, the drift coefficient first becomes significant at small pitch angles due to anomalous phase trapping and positive phase bunching, and then phase trapping and phase bunching occur at intermediate and large pitch angles.

The EMIC wave-induced proton scattering is one of the major processes responsible for ring current flux dropout and decay, energy coupling among different particle populations, and proton precipitation forming proton aurorae (see the review by Jordanova (2020)). The potential nonlinear interactions are not yet incorporated into the present ring current modeling on a global scale. Our study suggests that the quasilinear and nonlinear effects of proton scattering by EMIC waves are qualitatively similar to the interaction features seen in the analogous interaction between electrons and whistler-mode chorus waves (e.g., Gan, Li, Ma, Albert, et al., 2020), despite the significant differences in timescales and wave properties. The ring current protons at 1 keV–1 MeV energies are nonrelativistic, so they do not experience relativistic turning acceleration, which is important for multi-MeV electron acceleration by chorus waves (Omura et al., 2007; Summers & Omura, 2007). Recent satellite observations with high resolutions provide increasing evidence for the operating nonlinear electron scattering by chorus waves (e.g., Gan, Li, Ma, Artemyev, & Albert, 2020), yet less attention has been paid to the observational evidence of nonlinear interaction between EMIC waves and ring current protons with energies in the range of 1 keV–1 MeV.

The EMIC waves in our study are assumed to be monochromatic waves with field-aligned propagation at $L = 5$. The EMIC wave amplitude threshold of quasilinear applicability is expected to be higher than 1 nT if a wave frequency bandwidth and a wave normal angle distribution are considered. It is possible that after multiple interactions with different wave fields, combined positive and negative advection effects result in pitch angle scattering with magnitude similar to the quasilinear diffusion over a long period. However, the EMIC waves could have coherent wave structures with a rising tone frequency spectrogram (e.g., Shoji et al., 2021). Future investigations of the proton interaction with coherent EMIC waves based on satellite observations are required to evaluate the importance of nonlinear effects in the Earth's ring current proton dynamics.

Data Availability Statement

The data presented in this study are available at the data repository (Ma et al., 2025).

Acknowledgments
We would like to acknowledge the NASA Grants 80NSSC24K0572, 80NSSC21K1312, 80NSSC24K0266, and the NSF Grant AGS-2225445. MH is supported by the Alexander von Humboldt Postdoctoral Research Fellowship. JB gratefully acknowledges NASA Grant 80NSSC20K1270.

References

Albert, J. M., Artemyev, A. V., Li, W., Gan, L., & Ma, Q. (2021). Models of resonant wave-particle interactions. *Journal of Geophysical Research: Space Physics*, *126*(6), e2021JA029216. https://doi.org/10.1029/2021JA029216

Allanson, O., Elsden, T., Watt, C., & Neukirch, T. (2022). Weak turbulence and quasilinear diffusion for relativistic wave-particle interactions via a markov approach. *Front. Astron. Space Sci.*, *8*, 805699. https://doi.org/10.3389/fspas.2021.805699

Allen, R. C., Zhang, J.-C., Kistler, L. M., Spence, H. E., Lin, R.-L., Klecker, B., et al. (2015). A statistical study of EMIC waves observed by cluster: 1. Wave properties. *Journal of Geophysical Research: Space Physics*, *120*(7), 5574–5592. https://doi.org/10.1002/2015JA021333

An, X., Artemyev, A., Angelopoulos, V., Zhang, X.-J., Mourenas, D., Bortnik, J., & Shi, X. (2024). Nonresonant scattering of energetic electrons by electromagnetic ion cyclotron waves: Spacecraft observations and theoretical framework. *Journal of Geophysical Research: Space Physics*, *129*(3), e2023JA031863. https://doi.org/10.1029/2023JA031863

Anderson, B. J., & Fuselier, S. A. (1994). Response of thermal ions to electromagnetic ion cyclotron waves. *Journal of Geophysical Research*, *99*(A10), 19413–19425. https://doi.org/10.1029/94JA01235

Artemyev, A. V., Mourenas, D., Zhang, X.-J., & Vainchtein, D. (2022). On the incorporation of nonlinear resonant wave-particle interactions into radiation belt models. *Journal of Geophysical Research: Space Physics*, *127*(9), e2022JA030853. https://doi.org/10.1029/2022JA030853

Artemyev, A. V., Neishtadt, A. I., Albert, J. M., Gan, L., Li, W., & Ma, Q. (2021). Theoretical model of the nonlinear resonant interaction of whistler-mode waves and field-aligned electrons. *Physics of Plasmas*, *28*(5), 052902. https://doi.org/10.1063/5.0046635

Bell, T. F. (1984). The nonlinear gyroresonance interaction between energetic electrons and coherent VLF waves propagating at an arbitrary angle with respect to the Earth's magnetic field. *Journal of Geophysical Research*, *89*(A2), 905–918. https://doi.org/10.1029/JA089iA02p00905

Blum, L., Koval, A., Richardson, I., Wilson, L., Malaspina, D., Greeley, A., & Jaynes, A. (2021). Prompt response of the dayside magnetosphere to discrete structures within the sheath region of a coronal mass ejection. *Geophysical Research Letters*, *48*(11), e2021GL092700. https://doi.org/10.1029/2021GL092700

Bortnik, J., Albert, J. M., Artemyev, A., Li, W., Jun, C.-W., Grach, V. S., & Demekhov, A. G. (2022). Amplitude dependence of nonlinear precipitation blocking of relativistic electrons by large amplitude EMIC waves. *Geophysical Research Letters*, *49*(12), e2022GL098365. https://doi.org/10.1029/2022GL098365

Bortnik, J., Thorne, R. M., & Inan, U. S. (2008). Nonlinear interaction of energetic electrons with large amplitude chorus. *Geophysical Research Letters*, *35*(21), L21102. https://doi.org/10.1029/2008GL035500

Bortnik, J., Thorne, R. M., & Omidi, N. (2010). Nonlinear evolution of EMIC waves in a uniform magnetic field: 2. Test-Particle scattering. *Journal of Geophysical Research*, *115*(A12), A12242. https://doi.org/10.1029/2010JA015603

Cao, X., Ni, B., Liang, J., Xiang, Z., Wang, Q., Shi, R., et al. (2016). Resonant scattering of central plasma sheet protons by multiband EMIC waves and resultant proton loss timescales. *Journal of Geophysical Research: Space Physics*, *121*(2), 1219–1232. https://doi.org/10.1002/2015JA021933

Cao, X., Ni, B., Summers, D., Shprits, Y. Y., Gu, X., Fu, S., et al. (2019). Sensitivity of EMIC wave-driven scattering loss of ring current protons to wave normal angle distribution. *Geophysical Research Letters*, *46*(2), 590–598. https://doi.org/10.1029/2018GL081550

Capannolo, L., Li, W., Ma, Q., Shen, X.-C., Zhang, X.-J., Redmon, R. J., et al. (2019). Energetic electron precipitation: Multi-event analysis of its spatial extent during EMIC wave activity. *Journal of Geophysical Research: Space Physics*, *124*(4), 2466–2483. https://doi.org/10.1029/2018JA026291

Capannolo, L., Li, W., Ma, Q., Zhang, X.-J., Redmon, R. J., Rodriguez, J. V., et al. (2018). Understanding the driver of energetic electron precipitation using coordinated multisatellite measurements. *Geophysical Research Letters*, *45*(14), 6755–6765. https://doi.org/10.1029/2018GL078604

Chen, L., Thorne, R. M., & Horne, R. B. (2009). Simulation of EMIC wave excitation in a model magnetosphere including structured high-density plumes. *Journal of Geophysical Research*, *114*(A7), A07221. https://doi.org/10.1029/2009JA014204

Clilverd, M., Duthie, R., Hardman, R., Hendry, A. T., Rodger, C. J., Raita, T., et al. (2015). Electron precipitation from EMIC waves: A case study from 31 May 2013. *Journal of Geophysical Research: Space Physics*, *120*(5), 3618–3631. https://doi.org/10.1002/2015JA021090

Daglis, I. A., Thorne, R. M., Baumjohann, W., & Orsini, S. (1999). The terrestrial ring current: Origin, formation, and decay. *Reviews of Geophysics*, *37*(4), 407–438. https://doi.org/10.1029/1999RG900009

Denton, R. E., Goldstein, J., Menietti, J. D., & Young, S. L. (2002). Magnetospheric electron density model inferred from Polar plasma wave data. *Journal of Geophysical Research*, *107*(A11), 1386. https://doi.org/10.1029/2001JA009136

Drozdov, A. Y., Shprits, Y. Y., Usanova, M. E., Aseev, N. A., Kellerman, A. C., & Zhu, H. (2017). EMIC wave parameterization in the long-term VERB code simulation. *Journal of Geophysical Research: Space Physics*, *122*(8), 8488–8501. https://doi.org/10.1002/2017JA024389

Drozdov, A. Y., Usanova, M. E., Hudson, M. K., Allison, H. J., & Shprits, Y. Y. (2020). The role of hiss, chorus, and EMIC waves in the modeling of the dynamics of the multi-MeV radiation belt electrons. *Journal of Geophysical Research: Space Physics*, *125*(9), e2020JA028282. https://doi.org/10.1029/2020JA028282

Engebretson, M. J., Posch, J. L., Braun, D. J., Li, W., Ma, Q., Kellerman, A. C., et al. (2018). EMIC wave events during the four GEM QARBM challenge intervals. *Journal of Geophysical Research: Space Physics*, *123*(8), 6394–6423. https://doi.org/10.1029/2018JA025505

Fraser, B. J. (1985). Observations of ion cyclotron waves near synchronous orbit and on the ground. *Space Science Reviews*, *42*(3), 357–374. https://doi.org/10.1007/BF00214993

Frey, H. U., Haerendel, G., Mende, S. B., Forrester, W. T., Immel, T. J., & Ostgaard, N. (2004). Subauroral morning proton spots (SAMPS) as a result of plasmapause-ring-current interaction. *Journal of Geophysical Research*, *109*(A10), A10305. https://doi.org/10.1029/2004JA010516

Fu, S., Ni, B., Li, J., Zhou, C., Gu, X., Huang, S., et al. (2016). Interactions between magnetosonic waves and ring current protons: Gyroaveraged test particle simulations. *Journal of Geophysical Research: Space Physics*, *121*(9), 8537–8553. https://doi.org/10.1002/2016JA023117

Gan, L., Li, W., Albert, J. M., Hanzelka, M., Ma, Q., & Artemyev, A. (2025). Inhomogeneity ratio for nearly field-aligned electrons interacting with whistler-mode waves. *Geophysical Research Letters*, *52*(2), e2024GL111886. https://doi.org/10.1029/2024GL111886

Gan, L., Li, W., Hanzelka, M., Ma, Q., Albert, J. M., & Artemyev, A. V. (2023). Electron precipitation caused by intense whistler-mode waves: Combined effects of anomalous scattering and phase bunching. *Front. Astron. Space Sci.*, *10*, 1322934. https://doi.org/10.3389/fspas.2023.1322934

Gan, L., Li, W., Ma, Q., Albert, J. M., Artemyev, A. V., & Bortnik, J. (2020). Nonlinear interactions between radiation belt electrons and chorus waves: Dependence on wave amplitude modulation. *Geophysical Research Letters*, *47*(4), e2019GL085987. https://doi.org/10.1029/2019GL085987

Gan, L., Li, W., Ma, Q., Artemyev, A. V., & Albert, J. M. (2020). Unraveling the formation mechanism for the bursts of electron butterfly distributions: Test particle and quasilinear simulations. *Geophysical Research Letters*, *47*(21), e2020GL090749. https://doi.org/10.1029/2020GL090749

Gary, S. P., Thomsen, M. F., Yin, L., & Winske, D. (1995). Electromagnetic proton cyclotron instability: Interactions with magnetospheric protons. *Journal of Geophysical Research*, *100*(A11), 21961–21972. https://doi.org/10.1029/95JA01403

Hanzelka, M., Li, W., & Ma, Q. (2023). Parametric analysis of pitch angle scattering and losses of relativistic electrons by oblique EMIC waves. *Front. Astronomy Space Sci.*, *10*, 1163515. https://doi.org/10.3389/fspas.2023.1163515

Hanzelka, M., Li, W., Ma, Q., Qin, M., Shen, X.-C., Capannolo, L., & Gan, L. (2023). Full-wave modeling of EMIC wave packets: Ducted propagation and reflected waves. *Front. Astron. Space Sci.*, *10*, 1251563. https://doi.org/10.3389/fspas.2023.1251563

Hanzelka, M., Shprits, Y., Wang, D., Haas, B., Santolík, O., & Gan, L. (2025). Effects of fine spectral structure of chorus emissions on nonlinear scattering and acceleration of radiation belt electrons. *Journal of Geophysical Research: Space Physics*, *130*(4), e2024JA033382. https://doi.org/10.1029/2024JA033382

Horne, R. B., & Thorne, R. M. (1990). Ion cyclotron absorption at the second harmonic of the oxygen gyro-frequency. *Geophysical Research Letters*, *17*(12), 2225–2228. https://doi.org/10.1029/GL017i012p02225

Immel, T. J., Mende, S. B., Frey, H. U., Peticolas, L. M., Carlson, C. W., Gerard, J.-C., et al. (2002). Precipitation of auroral protons in detached arcs. *Geophysical Research Letters*, *29*(11), 1519. https://doi.org/10.1029/2001GL013847

Inan, U. S., Bell, T. F., & Helliwell, R. A. (1978). Nonlinear pitch angle scattering of energetic electrons by coherent VLF waves in the magnetosphere. *Journal of Geophysical Research*, *83*(A7), 3235–3253. https://doi.org/10.1029/JA083iA07p03235

Jacobs, J. A. (1970). *Geomagnetic micropulsations* (p. 15). Springer. https://doi.org/10.1007/978-3-642-86828-3

Jordanova, V. K. (2020). In V. K. Jordanova, R. Ilie, & M. W. Chen (Eds.), *Chapter 6 - ring current decay, ring current investigations* (pp. 181–223). Elsevier. https://doi.org/10.1016/B978-0-12-815571-4.00006-8

Jordanova, V. K., Farrugia, C. J., Thorne, R. M., Khazanov, G. V., Reeves, G. D., & Thomsen, M. F. (2001). Modeling ring current proton precipitation by electromagnetic ion cyclotron waves during the May 14–16, 1997, storm. *Journal of Geophysical Research*, *106*(A1), 7–22. https://doi.org/10.1029/2000JA002008

Jordanova, V. K., Kozyra, J. U., Nagy, A. F., & Khazanov, G. V. (1997). Kinetic model of the ring current-atmosphere interactions. *Journal of Geophysical Research*, *102*(A7), 14279–14291. https://doi.org/10.1029/96JA03699

Jordanova, V. K., Spasojevic, M., & Thomsen, M. F. (2007). Modeling the EMIC wave-induced formation of detached subauroral proton arcs. *Journal of Geophysical Research*, *112*, A08209. https://doi.org/10.1029/2006JA012215

Keika, K., Kistler, L. M., & Brandt, P. C. (2013). Energization of O+ ions in the Earth's inner magnetosphere and the effects on ring current buildup: A review of previous observations and possible mechanisms. *Journal of Geophysical Research: Space Physics*, *118*(7), 4441–4464. https://doi.org/10.1002/jgra.50371

Kitahara, M., & Katoh, Y. (2019). Anomalous trapping of low pitch angle electrons by coherent whistler mode waves. *Journal of Geophysical Research: Space Physics*, *124*(7), 5568–5583. https://doi.org/10.1029/2019JA026493

Li, J., Bortnik, J., Xie, L., Pu, Z., Chen, L., Ni, B., et al. (2015). Comparison of formulas for resonant interactions between energetic electrons and oblique whistler-mode waves. *Physics of Plasmas*, *22*(5), 052902. https://doi.org/10.1063/1.4914852

Liu, Z. Y., Zong, Q. G., Rankin, R., Zhang, H., Wang, Y. F., Zhou, X. Z., et al. (2022). Simultaneous macroscale and microscale wave–ion interaction in near-earth space plasmas. *Nature Communications*, *13*(1), 5593. https://doi.org/10.1038/s41467-022-33298-6

Lyu, X., Jordanova, V. K., Engel, M., Tu, W., & Ma, Q. (2024). Quantifying the role of EMIC wave scattering during the 27 February 2014 storm by RAM-SCB simulations. *Journal of Geophysical Research: Space Physics*, *129*(7), e2024JA032606. https://doi.org/10.1029/2024JA032606

Lyu, X., Ma, Q., Tu, W., Li, W., & Capannolo, L. (2022). Modeling the simultaneous dropout of energetic electrons and protons by EMIC wave scattering. *Geophysical Research Letters*, *49*(20), e2022GL101041. https://doi.org/10.1029/2022GL101041

Ma, Q., Li, W., Bortnik, J., Hanzelka, M., Gan, L., Artemyev, A. V., & Shen, X.-C. (2025). Dataset for "diffusive and nonlinear scattering of ring current protons by electromagnetic ion cyclotron waves in the Earth's inner magnetosphere" [Dataset]. *figshare*. https://doi.org/10.6084/m9.figshare.28780586

Ma, Q., Li, W., Thorne, R. M., Ni, B., Kletzing, C. A., Kurth, W. S., et al. (2015). Modeling inward diffusion and slow decay of energetic electrons in the Earth's outer radiation belt. *Geophysical Research Letters*, *42*(4), 987–995. https://doi.org/10.1002/2014GL062977

Ma, Q., Li, W., Thorne, R. M., Nishimura, Y., Zhang, X., Reeves, G. D., et al. (2016). Simulation of energy-dependent electron diffusion processes in the Earth's outer radiation belt. *Journal of Geophysical Research: Space Physics*, *121*(5), 4217–4231. https://doi.org/10.1002/2016JA022507

Ma, Q., Li, W., Yue, C., Thorne, R. M., Bortnik, J., Kletzing, C. A., et al. (2019). Ion heating by electromagnetic ion cyclotron waves and magnetosonic waves in the Earth's inner magnetosphere. *Geophysical Research Letters*, *46*(12), 6258–6267. https://doi.org/10.1029/2019GL083513

Meredith, N. P., Horne, R. B., Kersten, T., Fraser, B. J., & Grew, R. S. (2014). Global morphology and spectral properties of EMIC waves derived from CRRES observations. *Journal of Geophysical Research: Space Physics*, *119*(7), 5328–5342. https://doi.org/10.1002/2014JA020064

Min, K., Liu, K., Bonnell, J. W., Breneman, A. W., Denton, R. E., Funsten, H. O., et al. (2015). Study of EMIC wave excitation using direct ion measurements. *Journal of Geophysical Research: Space Physics*, *120*(4), 2702–2719. https://doi.org/10.1002/2014JA020717

Miyoshi, Y., Sakaguchi, K., Shiokawa, K., Evans, D., Albert, J., Connors, M., & Jordanova, V. (2008). Precipitation of radiation belt electrons by EMIC waves, observed from ground and space. *Geophysical Research Letters*, *35*(23), L23101. https://doi.org/10.1029/2008GL035727

Mouikis, C. G., Kistler, L. M., Baumjohann, W., Lund, E. J., Korth, A., Klecker, B., et al. (2002). Equator-S observations of He+ energization by EMIC waves in the dawnside equatorial magnetosphere. *Geophysical Research Letters*, *29*(10), 74-1–74-4. https://doi.org/10.1029/2001GL013899

Nakamura, S., Omura, Y., Kletzing, C., & Baker, D. (2019). Rapid precipitation of relativistic electron by EMIC rising-tone emissions observed by the Van Allen Probes. *Journal of Geophysical Research: Space Physics*, *124*(8), 6701–6714. https://doi.org/10.1029/2019JA026772

Ni, B., Cao, X., Zou, Z., Zhou, C., Gu, X., Bortnik, J., et al. (2015). Resonant scattering of outer zone relativistic electrons by multiband EMIC waves and resultant electron loss time scales. *Journal of Geophysical Research: Space Physics*, *120*(9), 7357–7373. https://doi.org/10.1002/2015JA021466

Ni, B., Zhang, Y., & Gu, X. (2023). Identification of ring current proton precipitation driven by scattering of electromagnetic ion cyclotron waves. *Fundamental Research*, *3*(2), 257–264. https://doi.org/10.1016/j.fmre.2021.12.018

Omura, Y., Furuya, N., & Summers, D. (2007). Relativistic turning acceleration of resonant electrons by coherent whistler mode waves in a dipole magnetic field. *Journal of Geophysical Research*, *112*(A6), A06236. https://doi.org/10.1029/2006JA012243

Omura, Y., Miyashita, Y., Yoshikawa, M., Summers, D., Hikishima, M., Ebihara, Y., & Kubota, Y. (2015). Formation process of relativistic electron flux through interaction with chorus emissions in the Earth's inner magnetosphere. *Journal of Geophysical Research: Space Physics*, *120*(11), 9545–9562. https://doi.org/10.1002/2015JA021563

Qin, M., Li, W., Nishimura, Y., Huang, S., Ma, Q., Hanzelka, M., et al. (2025). Sub-MeV electron precipitation driven by EMIC waves in plasmaspheric plumes at high L shells. *Journal of Geophysical Research: Space Physics*, *130*(3), e2025JA033756. https://doi.org/10.1029/2025JA033756

Remya, B., Halford, A. J., Sibeck, D. G., Murphy, K. R., & Fok, M.-C. (2023). Understanding quiet and storm time EMIC waves—Van Allen probes results. *Journal of Geophysical Research: Space Physics*, *128*(8), e2023JA031712. https://doi.org/10.1029/2023JA031712

Sakaguchi, K., Miyoshi, Y., Spanswick, E., Donovan, E., Mann, I. R., Jordanova, V., et al. (2012). Visualization of ion cyclotron wave and particle interactions in the inner magnetosphere via THEMIS-ASI observations. *Journal of Geophysical Research*, *117*(A10), A10204. https://doi.org/10.1029/2012JA018180

Sheeley, B. W., Moldwin, M. B., Rassoul, H. K., & Anderson, R. R. (2001). An empirical plasmasphere and trough density model: CRRES observations. *Journal of Geophysical Research*, *106*(A11), 25631–25641. https://doi.org/10.1029/2000JA000286

Shoji, M., Miyoshi, Y., Kistler, L. M., Asamura, K., Matsuoka, A., Kasaba, Y., et al. (2021). Discovery of proton hill in the phase space during interactions between ions and electromagnetic ion cyclotron waves. *Scientific Reports*, *11*(1), 13480. https://doi.org/10.1038/s41598-021-92541-0

Shoji, M., Miyoshi, Y., Omura, Y., Kistler, L. M., Kasaba, Y., Matsuda, S., et al. (2018). Instantaneous frequency analysis on nonlinear EMIC emissions: Arase observation. *Geophysical Research Letters*, *45*(24), 13199–13205. https://doi.org/10.1029/2018GL079765

Shprits, Y., Drozdov, A., Spasojevic, M., Kellerman, A. C., Usanova, M. E., Engebretson, M. J., et al. (2016). Wave-induced loss of ultra-relativistic electrons in the Van Allen radiation belts. *Nature Communications*, *7*(1), 12883. https://doi.org/10.1038/ncomms12883

Sigsbee, K., Kletzing, C. A., Faden, J., & Smith, C. W. (2023). Occurrence rates of electromagnetic ion cyclotron (EMIC) waves with rising tones in the Van Allen Probes data set. *Journal of Geophysical Research: Space Physics*, *128*(2), e2022JA030548. https://doi.org/10.1029/2022JA030548

Spasojevic, M., Frey, H. U., Thomsen, M. F., Fuselier, S. A., Gary, S. P., Sandel, B. R., & Inan, U. S. (2004). The link between a detached subauroral proton arc and a plasmaspheric plume. *Geophysical Research Letters*, *31*, L04803. https://doi.org/10.1029/2003GL018389

Staples, F. A., Ma, Q., Kellerman, A., Rae, I. J., Forsyth, C., Sandhu, J. K., & Bortnik, J. (2023). Differentiating between simultaneous loss drivers in Earth's outer radiation belt: Multi-dimensional phase space density analysis. *Geophysical Research Letters*, *50*(23), e2023GL106162. https://doi.org/10.1029/2023GL106162

Su, Z., Zhu, H., Xiao, F., Zheng, H., Zhang, M., Liu, Y. C.-M., et al. (2014). Latitudinal dependence of nonlinear interaction between electromagnetic ion cyclotron wave and terrestrial ring current ions. *Physics of Plasmas*, *21*(5), 052310. https://doi.org/10.1063/1.4880036

Summers, D., & Omura, Y. (2007). Ultra-relativistic acceleration of electrons in planetary magnetospheres. *Geophysical Research Letters*, *34*(24), L24205. https://doi.org/10.1029/2007GL032226

Thorne, R. M., & Horne, R. B. (1994). Energy transfer between energetic ring current H+ and O+ by electromagnetic ion cyclotron waves. *Journal of Geophysical Research*, *99*(A9), 17275–17282. https://doi.org/10.1029/94JA01007

Usanova, M. E., Drozdov, A., Orlova, K., Mann, I. R., Shprits, Y., Robertson, M. T., et al. (2014). Effect of EMIC waves on relativistic and ultrarelativistic electron populations: Ground-based and Van Allen Probes observations. *Geophysical Research Letters*, *41*(5), 1375–1381. https://doi.org/10.1002/2013GL059024

Wang, Z., Zhai, H., & Gao, Z. (2017). The effects of hydrogen band EMIC waves on ring current H+ ions. *Geophysical Research Letters*, *44*(23), 11722–11728. https://doi.org/10.1002/2017GL075843

Zhang, J.-C., Saikin, A. A., Kistler, L. M., Smith, C. W., Spence, H. E., Mouikis, C. G., et al. (2014). Excitation of EMIC waves detected by the van Allen Probes on 28 April 2013. *Geophysical Research Letters*, *41*(12), 4101–4108. https://doi.org/10.1002/2014GL060621

Zhang, X.-J., Li, W., Thorne, R. M., Angelopoulos, V., Bortnik, J., Kletzing, C. A., et al. (2016). Statistical distribution of EMIC wave spectra: Observations from van Allen Probes. *Geophysical Research Letters*, *43*(24), 12348–12355. https://doi.org/10.1002/2016GL071158

Zhang, Y., Paxton, L. J., Morrison, D., Wolven, B., Kil, H., & Wing, S. (2005). Nightside detached auroras due to precipitating protons/ions during intense magnetic storms. *Journal of Geophysical Research*, *110*(A2), A02206. https://doi.org/10.1029/2004JA010498

Zhou, S., & Cai, Y. (2024). Influence of initial proton energy on the nonlinear interactions between ring current protons and He+ band EMIC waves. *Journal of Geophysical Research: Space Physics*, *129*(10), e2024JA032954. https://doi.org/10.1029/2024JA032954

Zhu, H., Su, Z., Xiao, F., Zheng, H., Shen, C., Wang, Y., & Wang, S. (2012). Nonlinear interaction between ring current protons and electromagnetic ion cyclotron waves. *Journal of Geophysical Research*, *117*(A12), A12217. https://doi.org/10.1029/2012JA018088